

Imaging synthesized phosphatidylserine incorporation in single liposomes

Adriana Calaça Serrão^{1,2,✉}

¹Departamento de Bioengenharia, Técnico Lisboa, Lisboa, Portugal

²Department of Bionanoscience, Kavli Institute of Nanoscience, Technische Universiteit Delft, Delft, Netherlands

Reconstituting lipid synthesis inside self-assembled lipid vesicles is fundamental to achieve growth and division of a bottom-up minimal cell. Detection of cell-free lipid synthesis encapsulated in liposomes has been successfully performed in bulk. However, the incorporation of the synthesized lipids in the membrane of single-vesicles has not been demonstrated yet. With this work, we aim to detect phospholipid incorporation within the liposome membrane. To test this, we encapsulated the genes of the Kennedy pathway for lipid synthesis in *Escherichia coli* except *psd*, together with the cell-free gene expression protein synthesis using recombinant elements (PURE) system. The liposomes were incubated with the enhanced green fluorescent protein (eGFP)-C2 domain of lactadherin (lactC2) protein probe, which has shown to bind specifically to phosphatidylserine (PS). By image analysis using confocal microscopy, we showed that there is clear colocalization of the eGFP signal with the membrane in the majority of liposomes and that, on average, 55% of lipid vesicles are enriched in PS. The time tracking of enriched liposomes allowed to have a rough estimate of the lipid synthesis and incorporation kinetics: between 3.1 and 5.7 hours. The quantification of the incorporated phospholipid levels on the membrane was not possible, since the characterization of the method revealed that there is not a linear correlation between fluorescence intensity and PS concentration. We believe this work demonstrates the membrane incorporation of intravesicular synthesized phospholipids and poses as an advance for future studies regarding the growth and division of a liposome-based artificial cell.

Keywords: bottom-up synthetic biology, minimal cell, lipid synthesis, confocal fluorescence microscopy, PURE system

Correspondence: adriana.serrao95@gmail.com

Introduction

Life, as we know it, is extremely complex. However, is this complexity essential for life? What is the minimal set of components that a system should have to be considered *alive*? Is it possible to create this minimal living system experimentally? The minimal cell can be defined as a system that has the minimal albeit sufficient structural components to be considered alive. There are currently several lines of action being researched to tackle its construction and that can overall be grouped in two approaches, the bottom-up and the top-down approach (1).

Approaches to the minimal cell

The top-down approach consists of simplifying an already

existing living system, e.g. removing non-essential genes, while maintaining viability. Most of the efforts are focused on achieving a minimal genome commonly performed by successive deletion, while using the chassis of the starting-point organism, with successful attempts reported recently (2). The major disadvantage of the top-down approach is that it does not necessarily allow for complete comprehension of each of the components. Alternatively, the bottom-up approach consists in pooling together essential purified macromolecules within a compartment. This way, all the components are defined and of known function. To tackle the bottom-up minimal cell, two lines of action have been explored: encapsulation of either externally purified over-expressed proteins or of a minimal genome and a cell-free expression system. In the latter, protein expression occurs within the compartment, resembling more closely natural organisms. The main disadvantage is that the knowledge of the current living organisms restricts the possibilities for a bottom-up approach.

Components of the minimal cell

The essential characteristics of living organisms can be detailed as **compartmentalization** of cellular function, presence of a **flow of information** and capacity of **proliferation** (3). This definition is based on the empirical analysis of contemporary organisms, but does not exclude other possible minimal cell setups with either artificial or natural components not yet described. In contemporary living cells, the flow of information relies in nucleic acids serving as coding and memory and in proteins as functional agents. The compartment, consisting of a phospholipid membrane in all known organisms, is responsible for providing cells with a boundary and selectively allow nutrients to enter the cell. Lastly, the proliferation comprises all the functions regarding growth, reproduction and evolution. This includes for instance lipid synthesis, DNA replication and cell division.

The approach developed in our lab consists of building a DNA-based cell compartmentalized by a phospholipid membrane. For this, we use cell-free expression systems, encapsulated inside liposomes. These are artificially produced vesicles composed of one or more phospholipid bilayers. The *in vitro* transcription-translation system used is the PURE system, composed of the recombinant proteins necessary for transcription, translation, aminoacylation and energy restoration, mostly purified from (*E.coli*) (4). The liposomes should also entrap a minimal genome which allows mainly for functions related with proliferation and maintenance of the flow

of information. It is envisioned that not only a protein based route can be used for cell division (using the FtsZ system for instance) but also a lipid synthesis based route that can lead to an unbalanced surface-to-volume ration and eventually scission (5). Phospholipid synthesis is concluded to be an important process involved in membrane generation and potentially in division.

Phospholipid synthesis

Phospholipids play an important function defining the permeable barrier of cells and constitute also the matrix of membrane-associated proteins. The diversity of both phospholipid morphology (on the headgroup level or alkyl chain composition) and distribution is known to influence many key cellular processes (6).

E.coli has been the standard model for the study of bacterial membrane lipids. In its membrane, three major lipids are accumulated: phosphatidylethanolamine (PE) (about 75%), phosphatidylglycerol (PG) (about 20%) and cardiolipin (CL) (about 5% or lower). The Kennedy pathway for the formation of phospholipids in *E.coli* is commonly implemented for artificial cell lipid synthesis studies (7).

Phosphatidic acid (PA), considered the global lipid precursor, is synthesized in two sequential steps, starting with the acylation of the *sn*-1 position of glycerol 3-phosphate (G3P), using acyl-coenzyme A (CoA) as a substrate and giving rise to lysophosphatidic acid (LPA). A second acylation is performed in the *sn*-2 position giving rise to PA (8). These reactions are catalyzed by glycerol 3-phosphate acyl transferase (GPAT) and lysophosphatidic acid acyltransferase (LPAAT), coded by *plsB* and *plsC*, respectively. The lipid cytidine diphosphate - diacylglycerol (CDP-DAG) is subsequently synthesized by the simultaneous dephosphorylation of cytidine triphosphate (CTP) to cytidine diphosphate (CDP) and attachment to PA as a headgroup (9). This lipid can follow two synthetic routes that modify its headgroup. One of the derived pathways leads to the synthesis of PS and PE and the other to the synthesis of PG and CL. To form PS, phosphatidylserine synthase A (PssA) condenses L-serine with CDP-DAG (10). The conversion of PS to PE is catalyzed by phosphatidylserine decarboxylase (Psd) and consists in the decarboxylation of the L-serine headgroup. On the other hand, CDP-DAG can also condense with G3P leading to the synthesis of phosphatidylglycerolphosphate (PGP) which is then dephosphorylated by phosphatidylglycerolphosphate A (PgpA) to yield PG. CL can be synthesized with two molecules of PG, by the enzyme cardiolipin synthase A (ClsA) (10).

Implementation of phospholipid synthesis in a minimal cell

To date some attempts have been made to stimulate liposome growth. In early attempts, phosphatidylcholine (PC) was produced in the presence of liposomes, encapsulating purified enzymes (GPAT, LPAAT, and two more specific enzymes for PC synthesis), isolated from pig liver (11). Recently there was also the encapsulation of all the purified enzymes needed for the production of PE and PG, from the fatty-acid precursors (9). Both of these efforts were done by feeding the

externally produced proteins. However, a paradigm based on cell-free gene expression seems more viable to achieve a truly synthetic minimal cell.

The production of phospholipids using an *in vitro* transcription translation (IVTT) system encapsulated inside liposomes was first done by Kuruma *et al.*, 2009 (12). In this work the GPAT and LPAAT were produced separately in the presence of liposomes. After the proteins were expressed, both extracts were pulled together and PA was detected, however, both enzymes failed to work in the same environment. In this case, gene expression and lipid synthesis were not integrated. Recently, the production of all the Kennedy pathway enzymes in bulk starting from G3P and acyl-CoA precursors with PURE system was reported (10). For the first time, the membrane incorporation of *in vesiculo* synthesized phospholipids was detected. The cell-free expression with PURE system of both GPAT and LPAAT was performed simultaneously inside liposomes and the membrane was enriched in PA. Since the publication of this work, a minimal genome with the seven Kennedy pathway genes was constructed (pGEMM 7.0) and the PE and PG could be detected with mass spectrometry (MS) (unpublished work by Duco Blanken and Dr. David Foschepoth).

However, all of the past work was done using bulk measurement methods, that analyze the whole population of liposomes. The project presently described is a follow-up of the previously done work, using imaging techniques that allow to follow single liposomes and investigate the incorporation of the produced lipids in the membrane.

Lipid imaging techniques

Microscopic visualization of lipids poses as a powerful technique that is complementary to mass-spectrometry-based analysis (13). Probes for lipid imaging can be classified in either fluorophore conjugated lipids or lipid-binding probes (13). Using the former is an adequate strategy to follow the movement and localization of the lipids. The major concern with this approach is that the attached molecules can lead to lipids with different chemical characteristics than the natural counterparts (13). On the other hand, lipid-binding probes consists of a group of fluorescently-tagged lipid-binding proteins. The major setbacks of this method is the varying affinity and specificity of the binding. For the lipids synthesized by *E.coli*, there are described protein probes for PA (like Sos1-PH (14) and Spo20p (15)), PE (like duramycin and cinnamycin peptides (16)) and PS (like Annexin V and the lactC2 (17)).

Even though all of the lipids described belong to the Kennedy pathway and have been synthesized inside liposomes, some probes are more relevant to our experimental set-up. Imaging PA would not allow to verify the majority of the Kennedy pathway. In the case of PE, the available probes (duramycin and cinnamycin) are small-peptides that induce morphological changes in the membrane and that are curvature-dependent (16), which would require the usage of smaller vesicles like small unilamellar vesicles (SUV) instead of giant unilamellar vesicles (GUV). However, such small vesicles do not allow to encapsulate the PURE system compo-

nents. For the reasons described, imaging PS is believed to be the best option. Even though this lipid it is not a desired end product for our lipid synthesis module, studying its incorporation can give insights about the remaining lipids synthesized. To do so, lactC2 was proved to have increased sensitivity and specificity when compared to Annexin V, having also no dependence on divalent ion presence. For these reasons, lactC2 poses as the best imaging probe option.

Lactadherin-C2 domain binding PS

Lactadherin, a 47 kDa glycoprotein, is known to specifically bind PS and has been used to image PS in phospholipid membranes, by fusing the protein domain with a fluorescent probe. The ligation to PS is stereospecific (to the L-form of serine motif) and calcium independent (18). The binding has affinity for highly curved membranes, but it is not curvature-dependent, as it was shown to happen in both SUV and GUV (18).

The sensitivity of is high, as quantities of PS as low as 0.03 mass% have been detected (18). However, the binding is only linear (in regards to the concentration of PS) for PS < 4 mol%, reaching a plateau at around 8 mol% (19). Previous studies suggest the nature of the binding is also not charge-dependent, since other anionic lipids were also tested (20).

The ultimate goal of this project was to detect the incorporation of the lipids synthesized inside liposomes by the enzymes expressed with the PURE system. To do this, lactC2 was used as a probe to bind PS and allow imaging of its incorporation.

Materials and Methods

Plasmid cloning

The plasmid containing *egfp* and *lactC2* genes was kindly provided as a gift from Sergio Grinstein (20). PCR reactions were performed to amplify both the plasmid backbone and the gene construct. Adequate primers were used for each fragment: for the amplification of backbone primers ChD 471(CCGCTGAGCAATAACTAGC) and ChD 850(GATGATGGCTGCTGCCCATATGTATATCTCTTCTTAAAGTTAAAC); for the amplification of the *egfp-lactC2*, primers ChD 848 (TATACATATGGGCAGCAGCCATCATCATCATCACAGCAGCGGCTGGTGCCGCGCGGCAGCCATATGGTGAGCAAGGGCGAGG) and ChD 849 (AACTCAGCTTCTTTCGGGCTTGTCTAACAGCCCAGCAGCTCC). The reaction was performed with 10 ng of template DNA, 1 U of Phusion High-Fidelity (HF) DNA Polymerase (New England Biolabs) in HF buffer, present in the enzyme kit and supplemented with 0.2 mM of dNTPs, 0.2 μ M of forward primer and 0.2 μ M of reverse primer in a final volume of 50 μ L. The composition of the PCR products was verified with an TAE agarose gel (1% w/v) using SybrSafe staining (Thermo Fisher). The fragments were excised from the gel and purified using the Promega Wizard SV Gel and PCR Clean-Up System kit.

The pET-11a backbone and eGFP-LactC2 genes were assembled using a Gibson assembly protocol. For 100 ng of backbone, the equimolar quantity of gene was used. In the 20 μ L total mixture volume, besides the DNA, both the enzymes (1.3×10^{-3} U/ μ L of T5 exonuclease, 2.5×10^{-2} U/ μ L of Phusion polymerase, 4.8 U/ μ L of Taq ligase) and the ISO Buffer were added. The assembly reaction was incubated at 50°C for 60min. After this time, 20 U/ μ L of

DpnI were added to digest methylated DNA left the mixture incubated for 15 min a 37°C. To have plasmid propagation, 25 ng of the construct obtained with Gibson assembly was transformed into 500 μ L of One Shot™ TOP10 chemically competent *E.coli* (ThermoFisher) cells using heat shock. The cells were after plated and incubated overnight at 37°C.

Plasmid verification was done through colony PCR and restriction enzyme digestion. For the former, a PCR reaction was performed with 0.5 units of GoTaq DNA Polymerase (Promega) in GoTaq Buffer supplemented primers and dNTPs. The primers used were ChD 25 (GATGCTGTAGGCATAGGCTTGG) and ChD 310 (GGATCTCGACGCTCTCCCTTATG) as a reverse. For the latter, 2.5 units of DraI and 2.5 units of StuI were mixed with 500ng of DNA, in a final volume of 20 μ L (both enzymes by New England Biolabs). The mixture was incubated at 37°C for 1h. For both techniques, the results were visualized in TAE agarose gel (1%).

The DNA extracted from the colonies was afterwards sequenced externally by Sanger sequencing (Macrogen). To 300 ng of plasmid DNA, 0.25 μ M of primer was added in a final volume of 10 μ L. The primers used were ChD 288 (CGATGCGTCCGGC) and ChD 25.

Protein overexpression and purification

The plasmid was transformed by heat shock into both *E. coli* Rosetta ER2566 cells (New England Biolabs) and Rosetta 2 (Novagen). A preculture was incubated overnight at 37°C in LB medium supplemented with ampicillin. After, the cultures were diluted in a ratio of 1:1000, and incubated at 37°C with agitation (200 rpm) until achieving an OD₆₀₀ of around 0.6. In this moment, the protein production was induced with 1 mM of isopropyl beta-D-1-thiogalactopyranoside (IPTG) and the cells were incubated at 30°C for 3h with agitation (200 rpm).

Afterwards, the cells were pelleted by centrifugation at 13000 rpm for 5 min. The pellet was resuspended in Buffer A (150 mM NaCl, 20 mM Tris (pH 7.5), 20 mM imidazole), and the cells disrupted by sonication. The sonication was carried with ten pulses of 10 s and 30s of interval, using 30% of amplitude. After centrifugation at 4°C for 15min and 13000 rpm, the clear supernatant contains cytosolic proteins.

The protein purification was done using Ni-NTA Spin Columns (Qiagen) following the supplier protocol. The column was equilibrated and washed with Buffer A and the protein eluted with Buffer B (150 mM NaCl, 20 mM Tris, 500 mM imidazole; pH 7.5). To exchange the buffer B to storing buffer (10 mM Hepes-KOH; pH 7.5), Zeba Spin Desalting Columns (ThermoFischer) were used following the supplier protocol. To visualize each step of protein expression and purification a 12% polyacrylamide resolving gel and the 4% stacking gel were made. To denature 15 μ L of protein sample plus 1 μ L Dithiothreitol (DTT) and 15 μ L Laemmli 2 \times Concentrate Loading Buffer (Sigma-Aldrich) were mixed and incubated at 95°C for 10 min. The gel was ran at 100V while samples were in the stacking gel and at 180V in the resolving gel. The running buffer was: 250mM Tris-HCl, 200mM glycine, 1% w/v SDS; pH 8.3.

The concentration was measured with a Bradford assay. Bradford reagent (Sigma-Aldrich) was dissolved 1:10 and 500 μ L of this dilution was mixed with 20 μ L of the protein. bovine albumin serum (BSA) was used as a standard in a range of seven concentrations from 0.25 mg/mL to 2 mg/mL. The standards were diluted with the Bradford reagent 1:10 and the protein solutions 1:2.5. Each of the samples was done in triplicate, including a milli-Q sample, and the absorbance at a wavelength of 595nm was measured by spectrophotometry.

DNA coding lipid synthesis enzymes

The genes for DOPS synthesis (*plsB*, *plsC*, *cdsA* and *pssA*) were used either in the form of individual PCR amplified constructs or in the linearized plasmid format (pGEMM 7.0). The pGEMM 7.0 plasmid consists of the pUC19 backbone containing *plsB*, *plsC*, *cdsA*, *pssA* and *psd* under the domain of the T7 polymerase promoter and the genes *pgpA* and under *pgsA* the domain of the SP6 polymerase promoter. The plasmid was already available in the lab, synthesized previously by Dr. David Foschepoth and Gemma van der Voort. The digestion was conducted with 5U of EcoRI and 10µg of plasmid DNA.

IVTT system

The PUREfrex 2.0 system (GeneFrontier Corporation, Japan) was used for gene expression inside liposomes. The kit consists of three separate solutions. Solution I is the feeding solution (containing aminoacids, NTPs, tRNAs etc.), Solution II contains the essential enzymes (T7 RNA polymerase, energy recycling system, etc.) and Solution III containing ribosomes. The PUREfrex 2.0 solution for a 20 µL reaction consists of 10 µL of Solution I, 1 µL of Solution II, 2 µL of Solution III and the linearized DNA. The supplemented DNA can be the individual genes (each in 1 nM), the pGEMM 7.0 linearized plasmid, or the gene synthesizing for the YFP protein, depending on the nature of the experiment. In the case of lipid synthesis experiments, the reaction was supplemented with the necessary precursors: 1 mM CTP, 0.5 mM G3P and 0.5 mM of L-serine. Beta-mercaptoethanol (5 mM) was added to provide a reducing environment for the GPAT enzyme and 0.75 U/µL of SUPERase (ThermoFischer) to inhibit possible contamination with RNases.

Precursor films

Oleoyl-CoA (Avanti Polar Lipids) is kept in aliquots of 0.5 mg/mL, dissolved in chloroform:methanol:water (80:20:2) and stored under argon. With adequate pipettes for high pressure vapour liquids (MICROMAN pipettes, Gilson), the volume corresponding to 100µM of oleoyl-CoA, in the final reaction mix, was transferred to a PCR tube. The organic solvents were evaporated at ambient temperature and pressure for 2h, leading to a dried precursor film.

Lipid-coated beads

To prepare lipid-coated beads, a mixture of 1,2-dioleoyl-sn-glycero-3-phosphocholine (DOPC) (50 mol%), 1,2-dioleoyl-sn-glycero-3-phosphoethanolamine (DOPE) (36 mol%), 1',3'-bis[1,2-dioleoyl-sn-glycero-3-phospho]-glycerol (18:1 CL) (2 mol%), 1,2-distearoyl-sn-glycero-3-phosphoethanolamine-N-[biotinyl(polyethylene glycol)-2000 (DSPE-PEG(2000)-biotin) (1 mass%) (all from Avanti Polar Lipids) and Texas Red 1,2-Dihexadecanoyl-sn-Glycero-3-Phosphoethanolamine (DHPE-TexasRed) (0.5 mass%) (Invitrogen), for a total mass of 2 mg, was assembled in a 10 mL round-bottom flask. The remaining 12% were variable between different combinations of PS and PG, depending on the nature of the experiments. To the mixture 0.4 of 100 mM rhamnose (Sigma-Aldrich) in methanol were added, to promote lipid film swelling. Afterwards, 0.6g of 212-300 µm glass beads (Sigma-Aldrich) were added and the organic solvent was removed by rotary evaporation at 200 mbar for 2h, followed by overnight desiccation. Both the lipid solutions in chloroform and the lipid-coated beads were stored under argon at -20°C. Before each use, the beads were redessicated for at least 30 min.

Preparation of GUVs by natural swelling

To prepare GUVs, 1 mg of lipid coated beads is added per µL of the solution desired to encapsulate - denominated swelling solution. The swelling solution contained the PURE system the DNA tem-

plate. In the experiments with the objective of verifying gene expression, the mYFP-LL-Spinach construct was encapsulated (21). The GUVs were formed by natural swelling of the lipids in the surface of the beads, during 2h in ice and protected from light to avoid photobleaching. Regular tumbling was provided to promote detachment of the GUVs. Four freeze-thaw cycles were applied by submerging the sample in liquid nitrogen and thawing on ice. Afterwards, 2 µL of the supernatant containing liposomes was transferred to 5.5µL of the solution desired to be outside the liposomes (feeding solution). The feeding solution composition depended on the experiment, usually having 0.3 vol% of PUREfrex 2.0 Solution I and 150 nM of eGFP-LactC2 protein, unless stated otherwise. To confine gene expression to the liposome lumen, RQ1 DNase (Promega) was added (0.07 U/µL of feeding solution). The remaining enzymes tested - Proteinase K and RNase I (both from Thermo Fischer) - were used in the same concentration.

LC-MS

Liquid chromatography of phospholipid samples was performed using a CSH C18 2.1*50mm, 1.7 µm column, mobile phase A (water with 0.05% ammonium hydroxide and 2 mM acetylacetone), and mobile phase B (% 2-propanol, 20% acetonitrile, 0.05% ammonium hydroxide and 2 mM acetylacetone). A triple-quad mass spectrometer was used to detect PE and PS phospholipids. Transitions were established based on previous work by Scott *et al.*, 2016 (10), and scanning measurements of pure standards. Synthesized phospholipids were distinguished from phospholipids present at the start of the reaction (as part of the liposome matrix) by incorporation of ¹³G3P, resulting in a 3 Da mass shift. Mass spectrometry data was analysed using the Agilent Masshunter Quantitative analysis program, which automatically integrates peaks corresponding to the transitions set in the method. The integrated peak intensities were analyzed with MATLAB. For each transition, the average integrated counts signal of two injections was determined.

Fluorescence confocal microscopy

The sample is prepared in custom-made imaging chambers with two holes drilled in a glass slide, a narrow (aprox. 3 mm) and a wide one (aprox. 5 mm). On one side, a cover slip was glued with NOA 61 glue (Norland Products), creating the two compartments. The narrow chamber was then incubated with 10µL of BSA:BSA-biotin (1mg/mL) for 10min and then Neutravidin (1mg/mL). After the immobilization, the surface was washed three times with milli-Q and the suspension containing both the liposomes and the feeding solution was transferred to this chamber. The wider chamber is filled with 15µL of water, to avoid evaporation of the sample. The compartment is closed with a silicone square and a cover slip. The sample is incubated at 37°C overnight to allow for expression of the genes and binding of the protein probe. Image acquisition was performed using a Nikon A1R Laser scanning confocal microscope with the the SR Apo TIRF 100x oil immersion objective. The following excitation/emission wavelengths were used: 488/509 nm (lactC2-eGFP) 514/540 nm (YFP), and 561/595 nm (Texas Red). The sample height was adjusted manually in order to capture the immobilized liposomes.

Image analysis

To determine lactC2-eGFP fluorescence intensity at the membrane automated image analysis has been applied. An algorithm was used to determine liposome lumina, based on the texas red membrane signal and searching for circular components. First the centroid and radius were determined for every detected liposome. Then, line profiles along a line from the centroid to 1.5 times the radius, for 63 different angles, were determined. For every line profile, the max-

imum, corresponding to the membrane intersection, was recorded, and then averaged with other angles to obtain the eGFP intensity of the membrane. In the experiments where lumen pixel intensity was computed, the same rationale to find liposomes was applied.

Statistical analysis

To compare distributions, a two-sample kolmogorov-kmirnov test was applied to the data. The test returns a decision for the null hypothesis that both samples belong to the same continuous distribution. The MATLAB inbuilt function *kstest2* was applied to perform this analysis. The output is 1 if the null hypothesis is rejected with a 5% significance and 0 otherwise.

Results

Protein probe binds specifically to PS-containing liposomes

In order to use eGFP-lactC2 to detect PS synthesized in liposomes, it is indispensable to know the characteristics of this imaging method. With this objective in mind, the approach focused on 1) assuring binding specificity to PS, in comparison to other phospholipids and 2) studying how binding correlates with PS and lactC2 concentrations.

To tackle the objective 1), liposomes were prepared with both the standard and modified composition (12% PS or 12% PG, respectively). In the feeding solution 150nM of eGFP-lactC2 was added. The samples were imaged with fluorescent confocal microscopy (Fig. 1 A) and the average pixel intensity across the rim of liposomes was extracted.

The green fluorescence signal of eGFP clearly colocalizes with the membrane in the sample with liposomes containing PS, in the micrographs. Moreover, when focusing on specific liposomes, the two fluorescence peaks of the line profile (Fig. 1 B), corresponding to the membrane, completely overlap in both channels. The sample without PS, however, has no colocalization of the eGFP signal with the membrane. The signal throughout the line profile is approximately constant and similar to the background value.

Furthermore, the rim intensity of the population of liposomes, for eGFP channel, in different fields of view was analysed (Fig. 1 C and D). The histogram shows a distribution of the intensities centered on 1000 for the liposomes containing PS, close to a order of magnitude higher than for liposomes that did not contain PS with little overlap of both distributions. Examining the box plot of the same data, the difference in the populations is also clear. The average rim intensity for the PS-containing liposomes analyzed is higher than the majority of liposomes of the standard composition.

To compare both distributions, a two-sample kolmogorov-kmirnov test was applied to the data. The test returns a decision for the null hypothesis that both samples belong to the same continuous distribution. The null hypothesis was rejected for this data, confirming the observations.

These results show that the protein probe binds specifically to liposomes containing PS and the binary behaviour validates this method as a promising tool for examining incorporation of synthesized PS.

To access objective 2), liposomes were incubated with varying concentrations of the probe and studied with the goal of determining the saturating concentration.

After analysis of the average rim intensity of a population of liposomes, it was verified that for high concentrations (700nM) the membrane signal of eGFP was as intense in liposomes containing PS as in liposomes without it (results not shown). This suggests non-specific binding of the probe in these range of concentrations. For this reason, the remaining experiments continued to be done with 150nM of eGFP-lactC2 which has shown to allow a binary response of the method.

PS expressed *in vesiculo* is incorporated in the membrane.

The key aim of this work is to detect the membrane incorporation of PS, synthesized inside liposomes by the enzymes expressed with the PURE system. The production and accumulation of PS using the PCR constructs for *plsB*, *plsC*, *cdsA* and *pssA*, PURE system and in the presence of liposomes of the standard composition was firstly verified using LC-MS (results not shown). Since the system produces and accumulates PS its detection and visualization with eGFP-lactC2 can be performed.

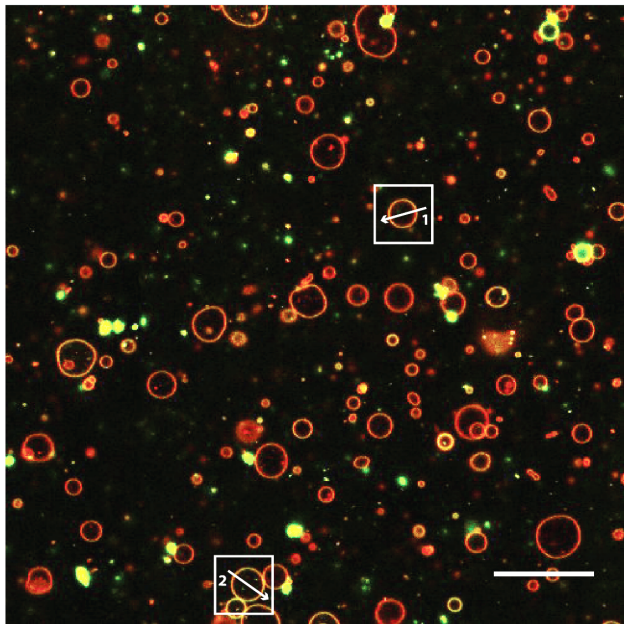
To do this, liposomes of the standard composition, encapsulating PURE system, lipid precursors and 1nM of linearized pGEMM 7.0 were incubated with DNase and 150nM eGFP-lactC2 in the feeding solution. DNase was used outside to restrict the gene expression to the lumen of liposomes. The negative controls used were: no feeding of oleoyl-Coenzyme A (o-CoA) and terminal protein (TP) DNA substituting the linearized plasmid.

The imaging method and image analysis employed were equivalent to the ones in the binding characterization experiment. Confocal micrographs are present in Fig. 2 A) and the extracted average rim intensity in Fig. 2 C). The percentage of enriched liposomes (Fig. 2 D) was computed by defining an enrichment threshold. This was done by fitting a normal distribution curve to the liposomes with 0% PS and extracting the eGFP pixel intensity for which 95% were not enriched.

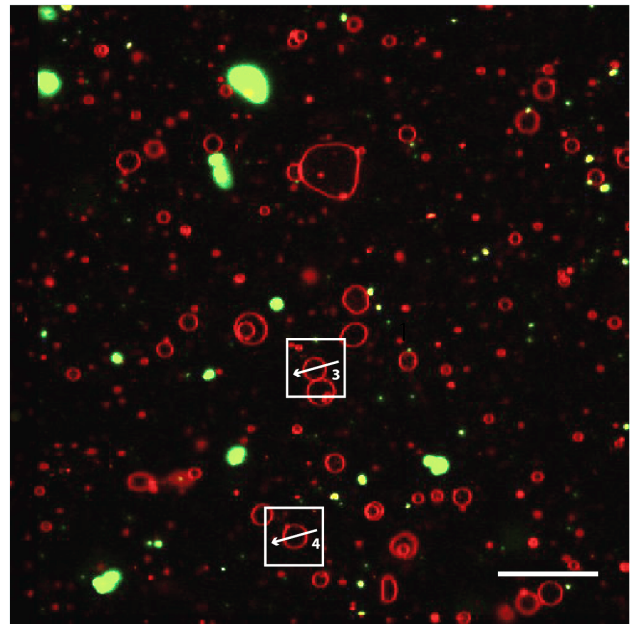
The positive sample shows a bright signal colocalized with the membrane of liposomes while the negative controls had no signal colocalization whatsoever. This is also clear from the analysis of single liposome line profiles (Fig 2 B). For the positive sample, there is overlapping of the membrane peaks in both channels. On the contrary, for the negative controls there are no significant peaks in the eGFP channel. The rim intensity median, for the positive sample (about 500 a.u.), is higher than the enrichment threshold defined ($T=422$ a.u.) in Section 1.4.1, and much higher than the median for the negative controls (150 a.u.). The percentage of enriched liposomes is on average 55%, considering three repeats of the experiment, and above 40% for all of them. In summary, PS synthesized inside liposomes is incorporated in the membrane and detected with the eGFP-lactC2 probe.

The number of theoretical enriched liposomes was predicted using a mathematical demonstration based on assumptions about the system. Since GUV were used in this project, calculations support that the large volumes of the vesicles allowed for encapsulation of all the components. PURE system, by itself, has over 80 different components, plus the DNA template and lipid precursors. All of these should be

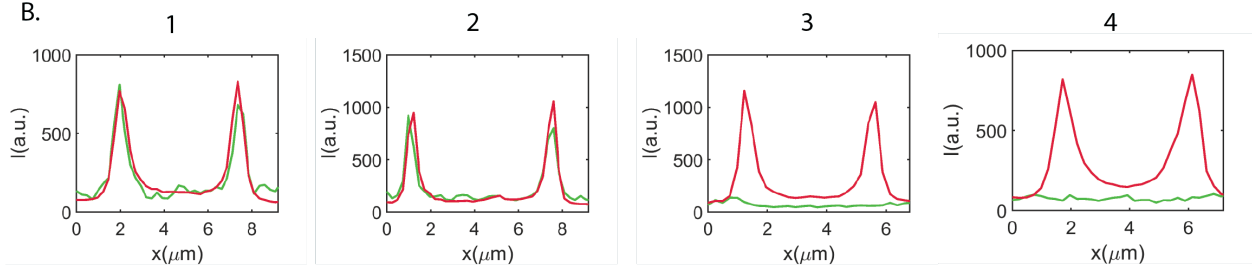
A. DOPC/**PS**/PE/CL liposomes



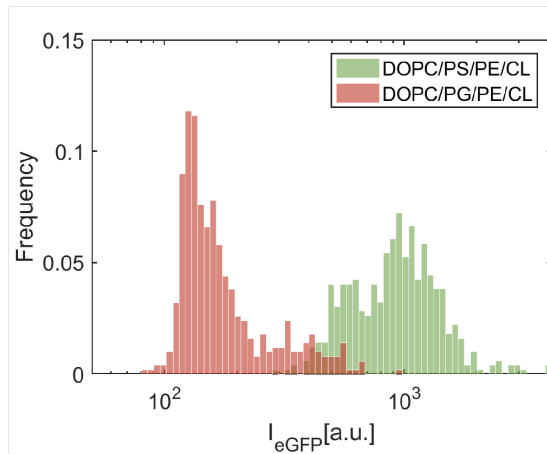
DOPC/**PG**/PE/CL liposomes



B.



C.



D.

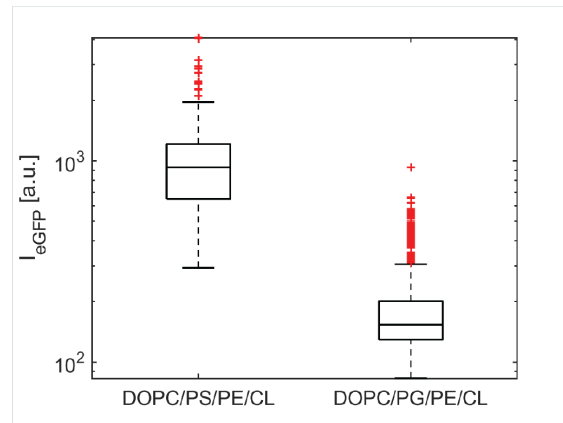


Fig. 1. Comparison of the lactC2 specificity between PS and PG. **A.** Confocal micrographs of liposomes (labelled in red) of different membrane compositions and incubated with 150 nM of eGFP-lactC2 outside (labelled in green). Scale bar is 20 μm . **B.** Line intensity profile for four liposomes (framed in **A.**), given that each of the colors represent the corresponding channel. **C.** Histogram and **D.** box plot displaying the distribution of average intensities across the rim of liposomes in the eGFP channel. Several liposomes ($n = [496, 500]$, respectively for the samples in the presented order) were taken into account.

present in concentrations high enough that lead to the production of a detectable amount of PS. The most unfavorable scenario was considered, using both the lowest concentration component (1 nM of DNA) and a lower than average vesicle radius (1 μm). The liposome volume corresponding to this radius equals to 4.2 fL, assuming complete sphericity. The average number of molecules of DNA expected to be

encapsulated is 2.5, for the referred concentration and volume. Considering that a Poisson distribution (Equation 1) describes molecule partitioning inside vesicles, the probability of having at least one molecule encapsulated is 0.918. The second least abundant component has a concentration of 15nM and an average number of molecules of 37.5. The computed probability of finding at least one molecule is \approx

1, applying the Poisson distribution centered around 37.5. Since the remaining components have a higher concentration, the probability of having at least one encapsulated molecule is 1 for all of them. Assuming independent encapsulation of each component, Equation 2 can be applied, where j is the number of events (in this case about 80 encapsulation events). As a result the final probability of encapsulating at least one molecule of each of the approximately 80 components is 0.918.

$$f(k; \lambda) = \frac{e^{-\lambda} \lambda^k}{k!} \quad (1)$$

$$P = \prod_1^j p_j \quad (2)$$

The values observed were lower than predicted as slightly more than half of liposomes were enriched, on average. We hypothesize this could be due to several reasons. Partitioning of some molecules in liposomes has shown not to follow necessarily a Poisson distribution. For instance, the aggregates formed by some of the molecules leads to liposomes with very high concentration of ribosomes or proteins (22). These interactions between components also challenges the assumption of independent encapsulation. It was verified that the complexes formed between DNA and other macromolecules can hinder transcription, and concluded that possibly only ca. 10% of the bulk DNA was transcriptionally active (23). On another perspective, for most processes more than only one molecule of each might be needed. It can be possible that some liposomes encapsulate all components but the necessary threshold concentration is not achieved or the relative concentrations between components do not allow reactions.

Moreover, the liposome-to-liposome variability can also be explained by differences in permeability. On one hand, if the probe does not access the inner leaflet and flip-flop does not occur, the liposome would not be stained even with incorporation of PS. On the other hand, if the liposome is permeable, DNase could also enter and degrade intra-vesicular pGEMM 7.0.

Kinetic of PS incorporation in the membrane of liposomes

Investigating the kinetic nature of the incorporation could elucidate on the time scale of gene expression, lipid synthesis and incorporation. To analyze this, the same experimental setup was used as with *in vesiculo* PS synthesis with the difference that incubation was performed in the microscope to allow frequent image acquisition.

After 15 hours of incubation, the end-point micrographs show liposomes enriched in PS Fig. 3 A. Micrographs of one enriched liposome through time show the increase in eGFP signal colocalized with the membrane (Fig. 3 B). The intensity of fluorescence increases through each of the close-ups, eventually achieving a plateau indicated by the similar intensity for six and fifteen hours. The close-up taken at 15h presents two smaller liposomes attached due to aggregation. Moreover, the radius of this liposome varied slightly during

imaging. Slight liposome movement during acquisition was often observed in both the positive samples and negative controls and was likely due to fluctuations on the imaged z-plane. The average rim intensity of the liposomes was extracted, for each time point. The curves of eGFP fluorescence over time, for three independent repeats, are shown in Fig. 4. A negative control without o-CoA was also performed and imaged at similar time-points. The liposomes of the positive sample showed a steep increase of fluorescence over time, followed by a plateau. The negative control displayed an approximately constant fluorescence, about one order of magnitude lower than the final intensity of the positive sample.

A sigmoid function was fitted to the average rim intensity of enriched liposomes, for each experimental repeat. The expression is shown Eq. 3, where B is the growth rate, k is the upper asymptote and t_f is the time corresponding to the inflection point. The parameters obtained for each repeat are presented in Table 1.

$$I = \frac{k}{1 + e^{-B(x-t_f)}} \quad (3)$$

The third repeat differs significantly from the other two. This repeat was done with a different stock of protein (produced with Rosetta 2 instead of Rosetta ER2566 cells) unlike all previous experiments. Possibly, a different fraction of protein was active and influenced the binding and fluorescence signal. In any case, a rough estimate of the time the system takes to produce and incorporate lipids can be extracted. The time to achieve the plateau can be estimated by doubling the t_f : between 3.1 and 5.7 hours.

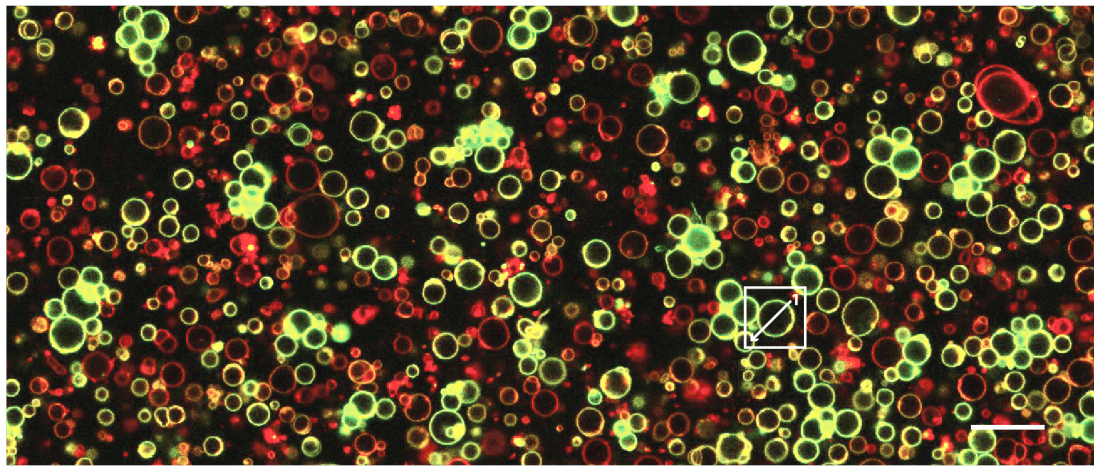
Table 1. Parameters of the sigmoid function fitted for each of the repeats.

	B (h^{-1})	k (a.u.)	t_f (h)
Repeat 1	0.90	1850	2.83
Repeat 2	0.73	1722	2.85
Repeat 3	1.84	1004	1.58

The lipid incorporation process comprises several steps: transcription and translation, incorporation or association of the enzymes with the membrane, lipid synthesis from precursors and incorporation of the phospholipid in the bilayer. In previous projects of our lab, the kinetic of the PURE system transcription and translation was characterized by expressing and measuring yellow fluorescent protein (YFP) fluorescence intensity inside single liposomes (unpublished work by Duco Blanken). It was concluded that gene expression achieved a plateau after about 5h for the PUREfrex 2.0 system.

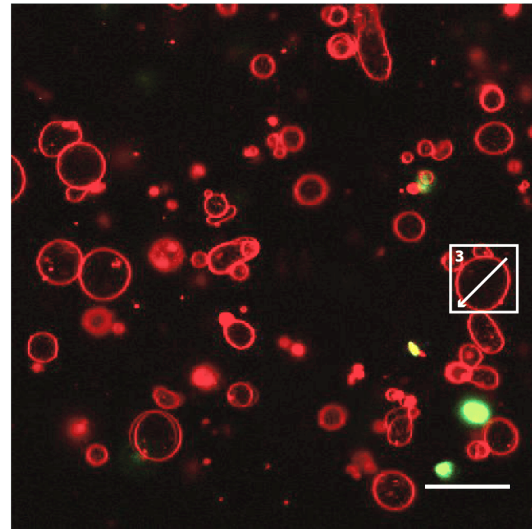
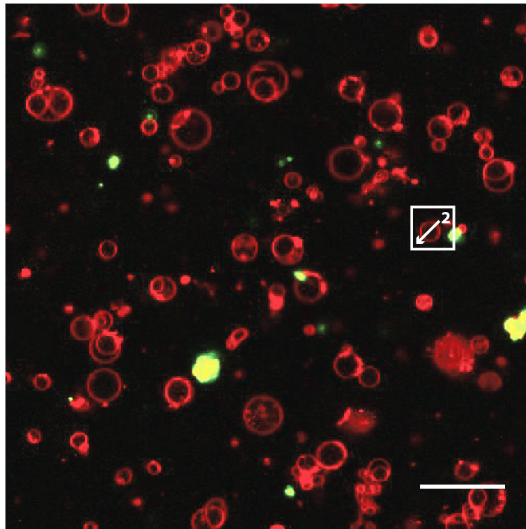
Even though it might not seem clear why gene expression takes longer to reach a plateau than lipid synthesis and incorporation, since for the latter there are more processes involved, these results are not necessarily incompatible. Firstly, all the sequential processes from transcription to phospholipid incorporation occur in parallel inside vesicles. That is, from the moment DNA is transcribed to mRNA (and a specific minimum threshold is achieved), translation can also start and so on. Combining this notion with the characteristics of our detection method, particularly the high sensitivity

A.

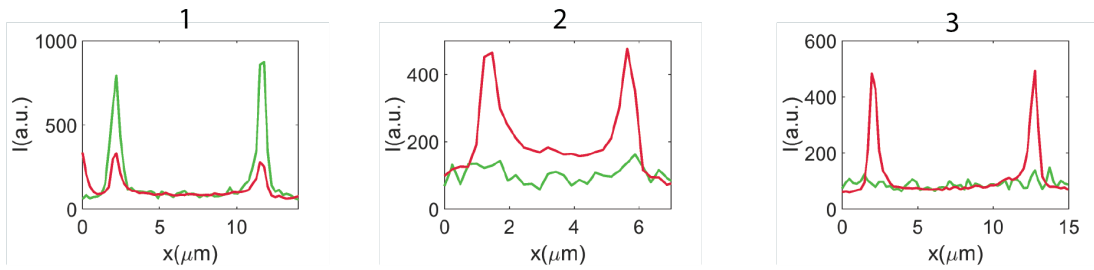


- oCoA

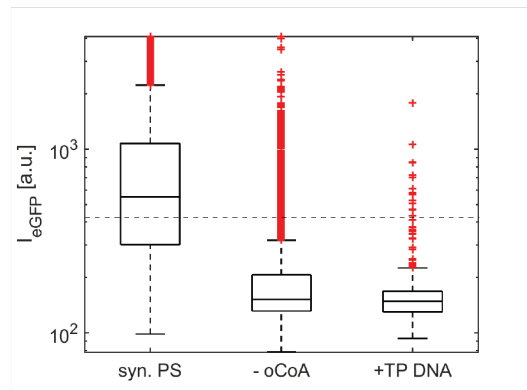
- genes + TP DNA



B.



C.



D.

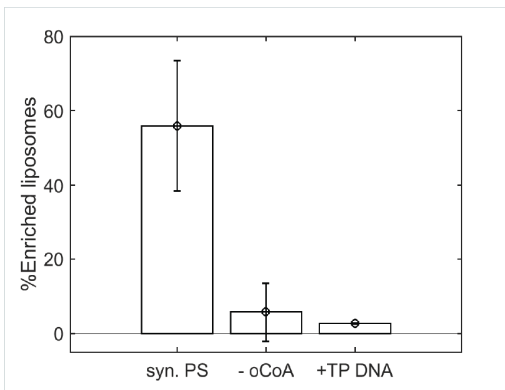
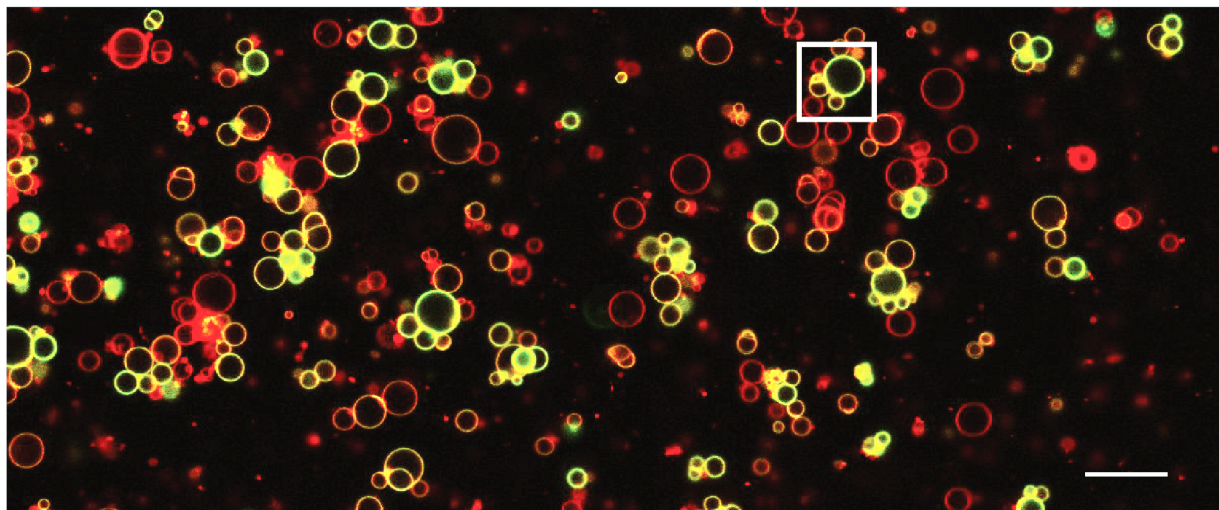


Fig. 2. Synthesized PS in liposomes with confined gene expression incorporates in the membrane of liposomes. **A.** Confocal micrographs of liposomes (labelled in red) encapsulating linearized pGEMM 7.0, PURE system, lipid precursors (G3P, CTP and L-serine) and incubated with 150 nM of eGFP-lac2 (labelled in green), $100\mu\text{M}$ of o-coA and DNase outside. Two negative controls are presented: (left) no o-CoA was fed to the system and (right) TP DNA was encapsulated instead of linearized pGEMM 7.0. Scale bar is $20\mu\text{m}$. **B.** Line intensity profile for three liposomes (framed in **A.**), given that each of the colors represent the corresponding channel. **C.** Distribution of average intensities across the rim of liposomes in the eGFP channel. The dashed line indicates the threshold used to consider a liposome enriched in PS. **D.** Percentage of PS-enriched liposomes for each sample. Four repeats of each sample were made, from which several liposomes ($n = [4048, 3642, 569]$, respectively for the samples in the presented order) were taken into account. The error bars represent the inter-sample standard deviation.

A.

15h



B.

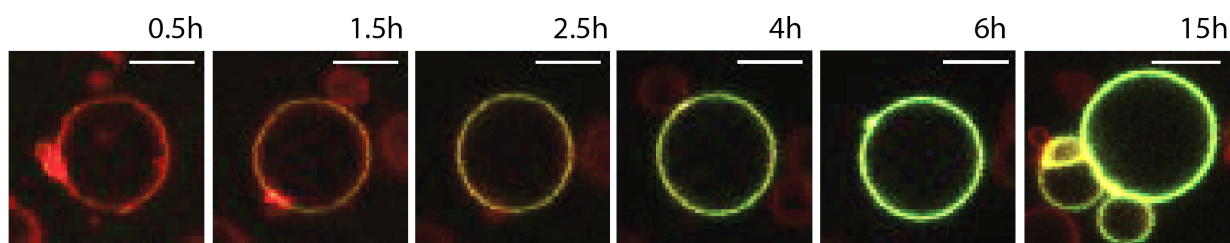


Fig. 3. Time-lapse of synthesized PS incorporation in liposomes. **A.** End-point confocal micrographs of liposomes (labelled in red) encapsulating linearized pGEMM 7.0, PURE system, L-serine and CTP, incubated with 150 nM of eGFP-lactC2 (labelled in green), 100 μ M of o-coA and 0.07U/ μ L DNase outside. Scale bar is 20 μ m. **B.** Single liposome (highlighted in **A.**) followed over time. Scale bar is 10 μ m.

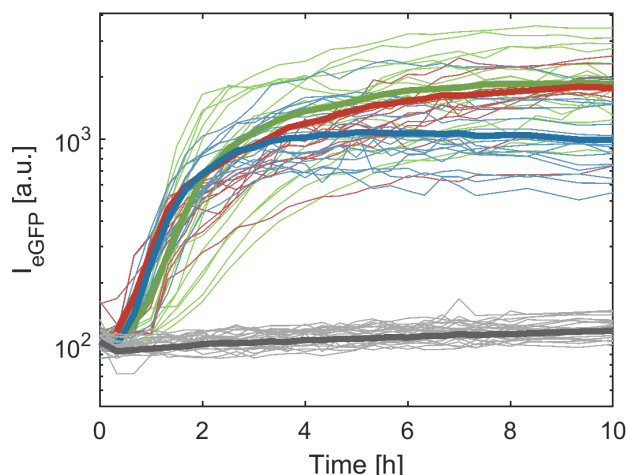


Fig. 4. Sigmoidal behaviour of fluorescence increase in enriched liposomes. The average rim intensity of liposomes was extracted over time. Each color is a different repeat (green, blue and red represent repeats of the positive sample) and grey represents a negative control without o-CoA. The thin lines corresponds to individual liposomes and the thick line corresponds to the average for the liposomes of the corresponding repeat. Several liposomes were analyzed : n=18 (green), n=12 (red), n=17 (blue), n=28 (grey).

of the method, it is understandable that the plateau for the signal of PS detection is lower than the plateau achieved for gene expression.

There were previous kinetic analysis of lipids synthesized by the enzymes expressed with the PURE system (10). These experiments were done by the expression of the GPAT and LPAAT enzymes in the presence of liposomes. Thus, the gene expression occurred in the extravesicular medium and the liposomes served as a membrane support for the lipids. After the lipid fraction was extracted and analyzed with MS (for each time-point). It was verified that the concentration plateau of PA was reached in 12h.

Comparatively, the results obtained in the present work suggest a much faster process. Since the past experiments were measured in bulk and in the expression occurred in the extravesicular solution, the contribution of the dilution of the components and the diffusion restraints can explain the comparative delay. The plateau of production can be achieved for a lower concentration of end-product when the experiment is done *in vesiculo*. Moreover, the work by Scott *et al.*, 2016, was done using PUREflex 1.0 (and not 2.0). Recently, it has been observed that PUREflex 2.0 has increased protein yield. With a higher concentration of enzymes produced in the same time-frame, the concentration threshold necessary to trigger lipid synthesis might be achieved earlier.

Our work detected PS presence, which corresponds to two more enzyme catalyzed steps when compared to the production of PA. However, each step does not correspond to a linear increase in the time needed to reach the plateau. Not only because the enzymatic steps occur in parallel but also because it was observed that the enzymes may work in tandem when incorporated simultaneously in the membrane, leading to higher plateau concentrations (10).

Conclusions

In this work we detect for the first time incorporation of phospholipids synthesized *in vesiculo*. Previous work done by our lab, in the scope of the lipid synthesis in the minimal cell, detected production of phospholipids using a bulk measurement method. Herein, we demonstrate the lipids synthesized incorporate in the membrane of liposomes, in a single-vesicle approach.

The incorporation of PS synthesized by enzymes expressed with the PURE system and confined to liposomes was imaged. We observed clear enrichment of 55% of the liposomes, on average. This not only demonstrates lipid synthesis and incorporation but also sets the technical ground to track PS enriched liposomes with different purposes.

The kinetic of lipid synthesis and incorporation was analyzed for enriched liposomes. As a rough estimate, the process takes up to 5.7 hours. Nevertheless, we observed a high variability, within sample (liposome-to-liposome) and within repeats (day-to-day). The current and past efforts of our lab to characterize and model the separate parts will allow for higher control and reproducibility in the future. Regarding the intra-sample variability, we reasoned macromolecule aggregation and intrinsic stochasticity of encapsulation could be the cause.

In the future, techniques to detect possible growth can be employed. These could be based on fluorophores that self-quench and, with growth, start having a fluorescent signal or, on the contrary, liposomes that contain both fluorescent energy transfer donor and acceptor lipid probes (e.g. rhodamine-PE and NBD-PE) and with the expansion, fluorescence intensity would decrease. Also, to allow deformation and division high quantities of lipid have to be produced. One of the ways currently being researched to lead to higher lipid yield is to expand the pathway to allow feeding the system with simpler precursors that are more water soluble and allow for higher initial concentrations. Better understanding and modelling of the PURE system dynamics will also reveal the most relevant parameters to manipulate in order for lipid yield improvement.

In conclusion, we believe this work demonstrated the membrane presence of the synthesized phospholipids and poses as an advance for future studies regarding liposome growth and division.

ACKNOWLEDGEMENTS

I want to thank Prof. Christophe Danelon for the opportunity to work in this lab and have this project, Duco Blanken and Dr. David Foschepoth for the daily supervision and Prof. Gabriel Monteiro for the supervision at Instituto Superior Técnico. Furthermore, I would like to thank the Erasmus Program for allowing me to have this

internship abroad and funding it. Finally I want to thank my family and friends for the constant support.

References

1. Pier Luigi Luisi. Toward the engineering of minimal living cells. *Anatomical Record*, 268(3): 208–214, 2002. ISSN 0003276X. doi: 10.1002/ar.10155.
2. Michael C Jewett and Anthony C Forster. Update on designing and building minimal cells. *Current Opinion in Biotechnology*, 21(5):697–703, 2010. ISSN 09581669. doi: 10.1016/j.copbio.2010.06.008.
3. Filippo Caschera and Vincent Noireaux. Integration of biological parts toward the synthesis of a minimal cell. *Current opinion in chemical biology*, 22:85–91, 2014. ISSN 18790402. doi: 10.1016/j.cbpa.2014.09.028.
4. Yoshihiro Shimizu, Takashi Kanamori, and Takuya Ueda. Protein synthesis by pure translation systems. *Methods*, 36(3):299–304, 2005. ISSN 10462023. doi: 10.1016/j.ymeth.2005.04.006.
5. Zohreh Nourian, Andrew Scott, and Christophe Danelon. Toward the assembly of a minimal divisome. *Systems and Synthetic Biology*, 8(3):237–247, 2014. ISSN 18725333. doi: 10.1007/s11693-014-9150-x.
6. W. Dowhan. MOLECULAR BASIS FOR MEMBRANE PHOSPHOLIPID DIVERSITY: Why Are There So Many Lipids? *Annual Review of Biochemistry*, 66(1):199–232, 1997. ISSN 0066-4154. doi: 10.1146/annurev.biochem.66.1.199.
7. Yi-Hsueh H Lu, Ziqiang Guan, Jinshi Zhao, and Christian R Raetz. Three phosphatidylglycerol-phosphate phosphatases in the inner membrane of *Escherichia coli*. *J. Biol. Chem.*, 286(7):5506–5518, 2011. ISSN 0021-9258. doi: 10.1074/jbc.M110.199265.
8. William Dowhan. A retrospective: Use of *Escherichia coli* as a vehicle to study phospholipid synthesis and function. *Biochimica et Biophysica Acta - Molecular and Cell Biology of Lipids*, 1831(3):471–494, 2013. ISSN 13881981. doi: 10.1016/j.bbalip.2012.08.007.
9. Marten Exterkate, Antonella Caforio, Marc C.A. Stuart, and Arnold J.M. Driessen. Growing Membranes *In Vitro* by Continuous Phospholipid Biosynthesis from Free Fatty Acids. *ACS Synthetic Biology*, 7(1):153–165, 2018. ISSN 21615063. doi: 10.1021/acssynbio.7b00265.
10. Andrew Scott, Marek J Noga, Paul De Graaf, Ilija Westerlaken, Esengul Yildirim, and Christophe Danelon. Cell-free phospholipid biosynthesis by gene-encoded enzymes reconstituted in liposomes. *PLoS ONE*, 11(10):1–23, 2016. ISSN 19326203. doi: 10.1371/journal.pone.0163058.
11. Peter Kurt Schmidli, Peter Schurtenberger, and Pier Luigi Luisi. Liposome-Mediated Enzymatic Synthesis of Phosphatidylcholine as an Approach to Self-Replicating Liposomes. *Journal of the American Chemical Society*, 113(21):8127–8130, 1991. ISSN 15205126. doi: 10.1021/ja00021a043.
12. Yutetsu Kuruma, Pasquale Stano, Takuya Ueda, and Pier Luigi Luisi. A synthetic biology approach to the construction of membrane proteins in semi-synthetic minimal cells. *Biochimica et Biophysica Acta - Biomembranes*, 1788(2):567–574, 2009. ISSN 00052736. doi: 10.1016/j.bbamem.2008.10.017.
13. M Maekawa and G D Fairn. Molecular probes to visualize the location, organization and dynamics of lipids. *Journal of Cell Science*, 127(22):4801–4812, 2014. ISSN 0021-9533. doi: 10.1242/jcs.150524.
14. Chen Zhao, Guangwei Du, Karl Skowronek, Michael A Frohman, and Dafna Bar-Sagi. Phospholipase D2-generated phosphatidic acid couples EGFR stimulation to Ras activation by Sos. *Nature Cell Biology*, 9(6):707–712, 2007. ISSN 14657392. doi: 10.1038/ncb1594.
15. M Bohdanowicz, D Schlam, M Hermansson, D Rizzuti, G D Fairn, T Ueyama, P Somerharju, G Du, and S Grinstein. Phosphatidic acid is required for the constitutive ruffling and macropinocytosis of phagocytes. *Molecular Biology of the Cell*, 24(11):1700–1712, 2013. ISSN 1059-1524. doi: 10.1091/mbc.E12-11-0789.
16. Kunihiko Iwamoto, Tomohiro Hayakawa, Motohide Murate, Asami Makino, Kazuki Ito, Tetsuro Fujisawa, and Toshihide Kobayashi. Curvature-dependent recognition of ethanolamine phospholipids by duramycin and cinnamycin. *Biophysical Journal*, 93(5):1608–1619, 2007. ISSN 00063495. doi: 10.1529/biophysj.106.101584.
17. Lasse N Waehrens, Christian W Heegaard, Gary E Gilbert, and Jan T Rasmussen. Bovine lactadherin as a calcium-independent imaging agent of phosphatidylserine expressed on the surface of apoptotic HeLa cells. *Journal of Histochemistry and Cytochemistry*, 57(10): 907–914, 2009. ISSN 00221554. doi: 10.1369/jhc.2009.953729.
18. Daniel E Otzen, Kristine Blans, Huabing Wang, Gary E Gilbert, and Jan T Rasmussen. Lactadherin binds to phosphatidylserine-containing vesicles in a two-step mechanism sensitive to vesicle size and composition. *Biochimica et Biophysica Acta - Biomembranes*, 1818(4): 1019–1027, 2012. ISSN 00052736. doi: 10.1016/j.bbamem.2011.08.032.
19. J Shi, S W Pipe, J T Rasmussen, C W Heegaard, and Gary E Gilbert. Lactadherin blocks thrombosis and hemostasis *in vivo*: Correlation with platelet phosphatidylserine exposure. *Journal of Thrombosis and Haemostasis*, 6(7):1167–1174, 2008. ISSN 15387933. doi: 10.1111/j.1538-7836.2008.03010.x.
20. Tony Yeung, Gary E. Gilbert, Jialan Shi, John Silvius, Andras Kapus, and Sergio Grinstein. Membrane phosphatidylserine regulates surface charge and protein localization. *Science*, 319(5860):210–213, 2008. ISSN 00368075. doi: 10.1126/science.1152066.
21. Pauline Van Nies, Alicia Soler Canton, Zohreh Nourian, and Christophe Danelon. *Monitoring mRNA and protein levels in bulk and in model vesicle-based artificial cells*, volume 550. Elsevier Inc., 1 edition, 2015. ISBN 9780128011232. doi: 10.1016/bs.mie.2014.10.048.
22. Tereza Pereira de Souza, Alfred Fahr, Pier Luigi Luisi, and Pasquale Stano. Spontaneous Encapsulation and Concentration of Biological Macromolecules in Liposomes: An Intriguing Phenomenon and Its Relevance in Origins of Life. *Journal of Molecular Evolution*, 79(5-6): 179–192, 2014. ISSN 00222844. doi: 10.1007/s00239-014-9655-7.
23. Zohreh Nourian and Christophe Danelon. Linking genotype and phenotype in protein synthesizing liposomes with external supply of resources. *ACS Synthetic Biology*, 2(4):186–193, 2013. ISSN 21615063. doi: 10.1021/sb300125z.